Nuclear Instruments and Methods in Physics Research A 378 (1996) 162–170

ELSEVIER

NUCLEAR INSTRUMENTS & METHODS IN PHYSICS RESEARCH Section A

Optical properties of an EMI K_2CsSb bialkali photocathode

M.E. Moorhead*, N.W. Tanner

Physics Department, University of Oxford, Keble Road, Oxford OX1 3RH, UK

Received 16 October 1995; revised form received 3 April 1996

Abstract

A measurement of the angular and polarisation dependence of the reflectance of an EMI 9124B K_2CsSb bialkali photocathode, with the photomultiplier immersed in water, has allowed an unambiguous determination of the K_2CsSb complex refractive index ($2.7 \pm 0.1 + i(1.5 \pm 0.1)$ at 442 nm wavelength) and thickness (23 ± 2 nm). The wavelength dependence of the refractive index has been obtained from a re-analysis of "three intensities" data from Timan [H. Timan, Optical characteristics and constants of high efficiency photoemitters, Revue Technique Thomson-CSF 8 (1976) 49]. A detailed study of K_2CsSb optical properties (absorptance, reflectance and transmittance) has been performed using the above results as reference points.

1. Introduction

The bialkali photocathode, K_2CsSb, is practically the universal choice for photomultipliers used for detecting scintillation and Cherenkov light. Its spectral sensitivity [1] is shown in Fig. 1. Most scintillators radiate in the region of 400 nm and Cherenkov light has a $1/\lambda^2$ spectrum. For many purposes the quantum efficiency, i.e. the fraction of the incident photons which release electrons from the cathode to the vacuum is the only cathode characteristic of interest. However, for nuclear, and in particular neutrino counters of large sensitive volume viewed by many photomultipliers, the dependence of the quantum efficiency on the angle of incidence and polarisation of the light, and the reflections from the photocathode, are matters of considerable importance.

The specific case which has stimulated the work described in this paper is the development of the solar neutrino detector for the Sudbury Neutrino Observatory [2]. It consists of 1000 m^3 of heavy water D_2O contained in a spherical acrylic vessel submerged in H_2O and viewed by 10000 photomultipliers. Each of these photomultipliers is equipped with a light reflecting concentrator [3]. The whole array of 10000 photomultipliers is supported by a spherical geodesic structure surrounding the D_2O and immersed in the H_2O. A neutrino interaction in the D_2O produces a relativistic electron whose Cherenkov radiation is detected by the array of photomultipliers. The energy, location, and direction of the electron is determined by the number, spatial distribution and time of arrival of the detected photons. The reconstruction of a neutrino event is complicated both by the angular dependence of the photomultiplier sensitivity and the detection of reflected photons.

The K_2CsSb bialkali photocathode has been known for forty years but there are no easily available published measurements of the angular dependence of reflections, nor of the angular dependence of the quantum efficiency. Timan [4] made measurements of reflections and transmission near normal incidence, over a range of wavelengths, for a variety of alkali antimonide photocathodes including K_2CsSb. Angular measurements have also been made for Cs_3Sb by

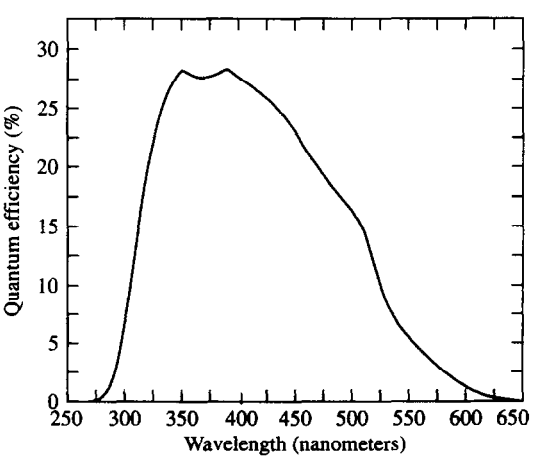

Fig. 1. Typical wavelength dependence of the quantum efficiency for a K_2CsSb bialkali photocathode on an EMI 9351B photomultiplier. The data were measured by Boardman [1] with equipment provided by the manufacturer. The cut-off at 300 nm is imposed by the glass envelopes; better glass which pushes the cut-off down to 280 nm is now available.

* Corresponding author. Present address: Lawrence Berkeley Laboratory, 1 Cyclotron Road, Berkeley, CA 94720, USA. Tel. +1 510 4867845, e-mail memoorhead@lbl.gov.

PII S0168-9002(96)00447-0

Greschat et al. [5] and Na_2KSb:Cs by Chyba and Mandel [6] which might be expected to serve as a guide to the likely behaviour of K_2CsSb. These measurements, Refs. [4–6], have all been made on photodiodes constructed solely for the purpose of studying the photocathode, whereas we are concerned with the photocathodes of production photomultipliers. In this case there is a multiplicity of stray reflections from the internal dynode structure and the aluminised surfaces, and light transmitted by the cathode is not accessible for measurement.

Since 1991 several authors have investigated bialkali photocathodes using production photomultipliers. Moorhead and Tanner [7] measured the angular dependence of the front reflectance of a bialkali photocathode using an EMI 9124B photomultiplier immersed in water and inferred from this measurement the complex refractive index and thickness of the photocathode. This method was then pursued by Lang [8] and by Lay [9] who made separate measurements on a pair of EMI 9125B photomultipliers. The results of all three authors are shown in Table 1 where there is good agreement in the real part of the measured complex refractive indices and reasonable agreement in the imaginary part. There is also good agreement in the deduced photocathode thicknesses for the two cases where different authors measured the same photomultiplier. However, as expected, different photomultipliers can have different K_2CsSb photocathode thicknesses.

Lay [9] has gone even further and demonstrated that the absorptivity of a bialkali photocathode, as calculated from its complex refractive index and thickness, has the same angular dependence as that of its quantum efficiency. The precision to which this agreement can be verified is limited to the few percent level by the difficulty in accounting for stray reflections inside the photomultiplier, but for most purposes, such as the characterization of photomultiplier responses in neutrino detectors, this precision is quite acceptable.

All of the above recent investigations [7–9] of bialkali photocathodes have been limited to the 442 nm wavelength of He–Cd lasers. The only published data at other wavelengths are those of Timan [4] which have been re-analysed in Section 4 of this paper to provide the wavelength dependence of the complex refractive index.

2. Reflections from a photocathode

For a K_2CsSb photocathode the most useful laser wavelength that falls in the sensitive range, see Fig. 1, is the He–Cd line at 442 nm, which is also a good match to the common scintillator wavelengths. All of the measurements have been made at 442 nm using a 10 mW Liconix He–Cd laser suitably attenuated to avoid damage to the photocathode.

The pattern of reflections from the neighborhood of the cathode of a photomultiplier are illustrated in Fig. 2 for the case of the glass window immersed in water. In air the maximum angle of incidence at the photocathode itself is $\theta_2(c) = \sin^{-1}(1/n_2) = 42.2°$ which is also the critical value of θ_2 for total internal reflection at the cathode/vacuum interface. For the photocathode properties the informative measurements are those for the reflected intensities at $\theta_2 > 42.2°$. Reflection measurements in air are of little value either for the practical properties of neutrino detectors or the parametrization of the properties of photocathodes.

The laser beam had a diameter of about 1.1 mm and a divergence of 0.5 mr which allowed the separation of multiple reflections related to the 2 mm thickness of the glass, see Fig. 2. Multiple reflections within the thickness of the photocathode, ~ 20 nm, completely overlapped and added coherently. Many other reflections, not shown in Fig. 2, from internal surfaces of the photomultiplier were observed but did not cause difficulty with the measurements of cathode reflections.

The intensity of the reflections from a K_2CsSb photocathode were measured as a function of the angle of incidence and polarization using a 30 mm EMI 9124B photomultiplier. A schematic plan view of the apparatus is shown in Fig. 3. The polarization of the laser beam is normally vertical, which is the TE mode or transverse electric (relative to the plane of reflection); it was rotated into the TM (transverse magnetic) mode by physically rotating the laser [1]. The beam intensity was continuously monitored with the beam-splitter (microscope slide) and photodiode arrangement. A Perspex [2] cylinder, of diameter 150 mm was located on a rotating table and centred on the vertical axis of rotation of the table. The photomultiplier tube was mounted through the side of the Perspex cylinder with the centre of its front win-

[1] This is not a recommended procedure for He–Cd lasers.

[2] Perspex is the trade name for ICI acrylic which has a sharp optical cut-off at 370 nm imposed by the UV stabiliser.

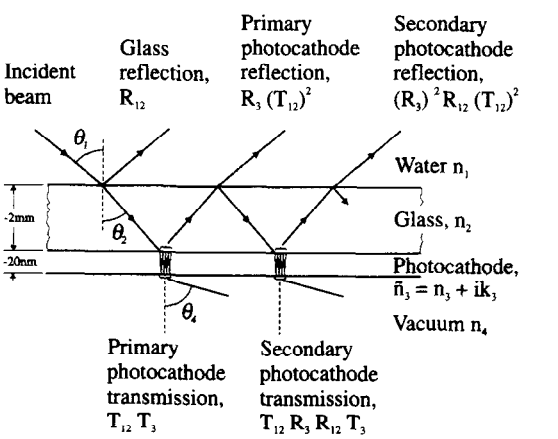

Fig. 2. The multiple reflections of a laser beam of diameter 1.1 nm which occur inside the glass window of the photomultiplier emerge parallel, separated by a distance of order 2 mm. By contrast, the multiple reflections which occur inside the thin (~ 20 nm) photocathode overlap each other and interfere coherently with each other. Their amplitudes must be summed, taking into account their relative phases, in order to calculate the total amplitudes of the reflected and transmitted waves.

Table 1
Measured bialkali photocathode refractive indices $n_3 + ik_3$ and thicknesses d at 442 nm wavelength

PMT type	Serial no.	Ref.	n_3	k_3	d [nm]
EMI 9124B	–	[7]	2.7 ± 0.1	1.5 ± 0.1	23 ± 2
EMI 9125B	6605	[8]	2.67 ± 0.07	1.69 ± 0.04	25.5 ± 1.0
EMI 9125B	6605	[9]	2.66 ± 0.04	1.74 ± 0.02	24.4 ± 0.6
EMI 9125B	6515	[8]	2.64 ± 0.06	1.57 ± 0.04	16.8 ± 0.7
EMI 9125B	6515	[9]	2.63 ± 0.02	1.59 ± 0.02	16.7 ± 0.3

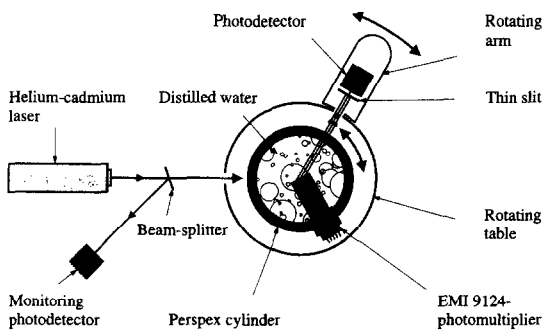

Fig. 3. Schematic representation of the apparatus used for photocathode reflection measurements.

dow at the axis of rotation of the table. The horizontal laser beam was aligned to be incident at the centre of the photomultiplier window. The Perspex cylinder was filled with deionized water, completely immersing the photomultiplier.

The photodiode on an independently rotating arm (with the same axis of rotation as the table) measured the intensity of the reflections from the photomultiplier. All the reflectance measurements were normalised to the beam intensity which was measured with the same rotating photodiode by withdrawing the photomultiplier from the centre and allowing the beam to pass straight through the Perspex cylinder. Both the straight-through beam and the photomultiplier reflections suffer the same losses from reflection at the Perspex cylinder. Hence these losses factor out upon normalization. However, a variable percentage of the beam was scattered by small defects on the Perspex cylinder. The r.m.s. fluctuation in the reflectance measurements caused by the passage *twice* through the walls of the scattering Perspex cylinder was measured from the r.m.s. fluctuation of the straight through beam which also passes *twice* through the Perspex. This r.m.s. fluctuation of $\pm 1.5\%$ was the limiting random error of the reflectance measurements. The nonlinearity of the photodiodes and any sensitivity to polarization was very much less than the fluctuation uncertainty.

The multiple reflections emerged parallel from the photomultiplier window, separated from one another by a distance of order 2 mm (the thickness of the window, see Fig. 2). Since the laser beam was 1.1 mm wide it was possible to resolve the multiple reflections into individual components: glass reflection, primary photocathode reflection, secondary photocathode reflection, etc. Moreover, the ability to resolve the multiple reflections was greatly enhanced by the focussing effect of the water-filled Perspex cylinder which acted as a thick cylindrical lens. This lens focussed the parallel laser beam into a vertical line at a distance $n_1 r/2(n_1 - 1) \simeq 2r$ from the centre of the lens where n_1 is the refractive index of water (1.34 at 442 nm) and r is the radius of the lens, i.e. the radius of the Perspex cylinder. Hence at a distance r from the Perspex cylinder the straight-through beam appeared as a vertical line and the multiple reflections as a series of parallel vertical lines. The focussing also caused the multiple reflections to converge together, but with only *half* the focussing power of the lens, since the multiple reflections were produced parallel to each other *inside* the lens. They were brought together at a distance $n_1 r/(n_1 - 1) \simeq 4r$ from the centre of the lens. Therefore at a distance r from the Perspex cylinder their separation had only decreased by a third from the initial ~ 2 mm whereas each individual reflection was focussed into a $\simeq 0.1$ mm wide line and hence could easily be resolved by placing a 0.15 mm wide vertical slit in front of the rotating photodiode, as in Fig. 3.

Measurements were made of both the glass reflectance R_g and the primary photocathode reflectance R_p as a function of the angle of incidence θ_1 at the photomultiplier window (see Fig. 2), for both polarizations independently, i.e. electric field vector perpendicular or parallel to the plane defined by the incident and the reflected beams, (respectively TE and TM waves). The measured primary photocathode reflection R_p is plotted in Fig. 4 where there is a marked and sensitive structure above the angle $\theta_1 = 48.3°$ which corresponds to the onset of total internal reflection at the cathode/vacuum boundary.

3. Analysis of reflectance

At a specific wavelength one may be able to parametrize the reflections and transmissions of a photocathode, Fig. 2, in terms of three parameters for the cathode, viz the real and imaginary parts of the refractive index, $\tilde{n}_3 = n_3 + ik_3$, and the thickness d; the refractive indices of the glass window n_2 and the external medium n_1 being given. Such a three parameter description is appropriate for a homogeneous cathode layer without any peculiar surface properties.

The reflected and transmitted intensities of Fig. 2 are ex-

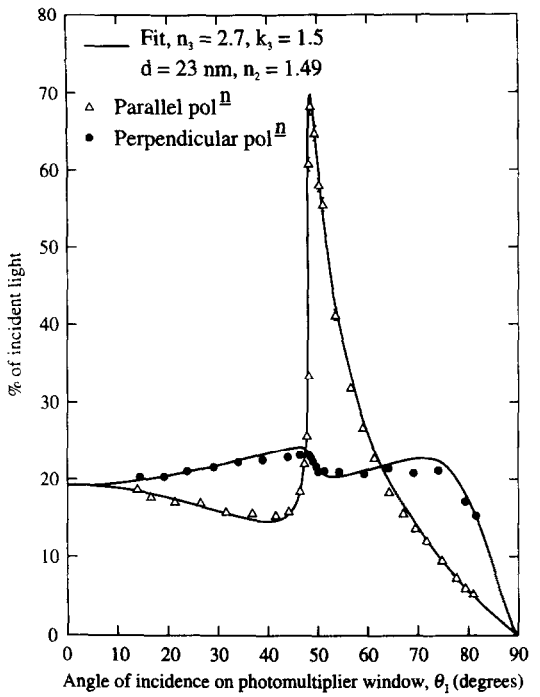

Fig. 4. Measured intensity of the primary photocathode reflection R_p as a function of angle of incidence θ_1 and polarization, TE and TM. The curves are the best fit of $R_3T_{12}^2$ to the data for free adjustment of the parameters n_2, n_3, k_3 and d. The geometry of the reflections is indicated in Fig. 2.

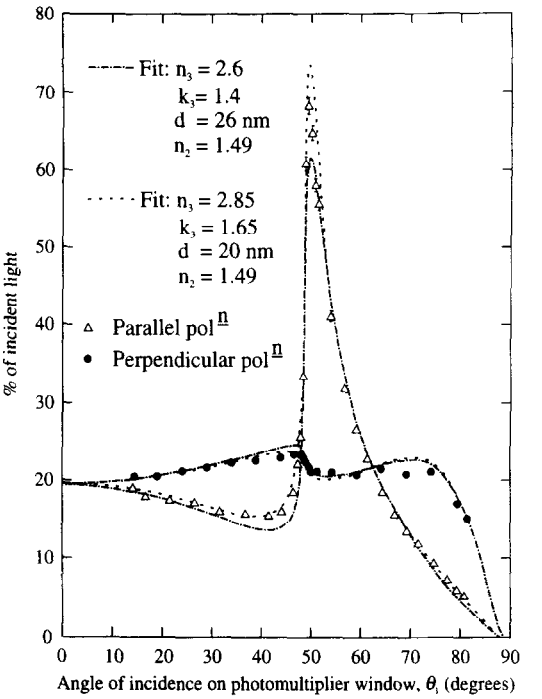

Fig. 5. Two fits to the primary photocathode data from the line in the 4D parameter space (n_2, n_3, k_3, d) along which Δ_{rms} increases the least quickly from its minimum as the normal incidence reflectance along this line is more or less constant. The parameter values of these fits have been obtained by minimizing Δ_{rms} for a fixed value of n_2 (1.49) and two fixed values of d (20 and 26 nm). The respective Δ_{rms} values are 5.5% and 5.9%.

pressed in terms of four quantities R_{12}, T_{12}, R_3 and T_3 which can be calculated as a function of angle for each polarization using the well known Fresnel formulae, e.g. see Ref. [10]. Essentially there are three unknowns n_3, k_3 and d to be determined by making a least squares fit of the calculated primary photocathode reflection $R_3T_{12}^2$ to the measured primary photocathode reflection R_p as a function of angle, see Figs. 2 and 4. The refractive index of the glass n_2 can be determined by fitting the calculated glass reflectance R_{12} to the measured glass reflectance R_g, but a consistent and more accurate value for n_2 was obtained by fitting the primary photocathode reflectance R_p with four variables, n_2, n_3, k_3, d.

The value of $R_3T_{12}^2$ was computed for both polarizations, TE and TM, and all experimental values of θ_1 (see Fig. 4) within the volume of the four dimensional parameter space defined by Table 2. The best fit of $R_3T_{12}^2$ to R_p occurred at $n_2 = 1.49$, $n_3 = 2.7$, $k_3 = 1.5$, $d = 23$ nm with an

Table 2
Four dimensional parameter space investigated in the least squares fit of the primary photocathode reflectance R_p

Parameter	Minimum	Maximum	Step size
n_2	1.475	1.495	0.005
n_3	1.0	6.0	0.05
k_3	0.0	5.0	0.05
d [nm]	5.0	50.0	0.5

RMS deviation from the 52 measured points of 3.6%. This is larger than the 1.5% quasi-statistical fluctuations imposed by the imperfections of the Perspex cylinder, Fig. 3, but not so large that one would reject the simple description of a photocathode in terms of a complex refractive index: uniformity of the cathode at the per cent level is not guaranteed and the area investigated changes with θ_1 by a few mm and a slightly different area may have been used for TE and TM polarizations.

The four parameters, n_2, n_3, k_3 and d, are separately strongly constrained by the RMS error of the fit, the error increasing steeply for a change in one of these variables. However there is a line in this four dimensional space characterized by approximately constant values of n_2, n_3/k_3, and $|\tilde{n}_3|^2 d$ along which the RMS error rises least steeply from the minimum, the calculated reflection $R_3T_{12}^2$ near normal incidence remaining constant. Fixing $n_2 = 1.49$ and $d = 20$ and 26 nm, either side of the best four parameter fit $d = 23$ nm (Fig. 4), provided the two parameter, n_3 and k_3, fits of Fig. 5. The RMS errors are respectively 5.5% and 5.9%, cf. 3.6% of Fig. 4, and in particular these fits do not reproduce the measured height of the peak in the TM polarized reflection.

From the photocathode's complex refractive index and thickness one can calculate the transmittance T_3 and reflectance R_3 as well as the absorptance A_3 using the relation

Table 3
Timan's measurements [4], at near normal incidence, of the transmittance, T, front reflectance (from the glass side), R_f, and back reflectance (from the vacuum side), R_v, of two K_2CsSb bialkali photocathodes labelled B1 and B3. The measurements are corrected for reflectance losses at all air/glass interfaces

Wavelength [nm]	T(B1)	R_f(B1)	R_v(B1)	T(B3)	R_f(B3)	R_v(B3)
390	0.145	0.23	0.44	0.135	0.25	0.435
453.5	0.19	0.275	0.455	0.155	0.315	0.46
505	0.30	0.29	0.41	0.26	0.30	0.41
601.5	0.465	0.235	0.295	0.445	0.27	0.33
798	0.715	0.185	0.195	0.695	0.22	0.23
897.5	0.80	0.15	-	0.775	0.19	-
1070	0.85	0.125	-	0.84	0.145	-
1153	0.87	0.115	0.115	0.865	0.125	0.125

$R_3 + T_3 + A_3 = 1$. Fig. 6 shows A_3 and T_3 for the EMI 9124B photomultiplier for both the TE and TM polarizations as a function of the angle of incidence at the glass/cathode interface.

4. Refractive index versus wavelength

Timan [4] has published measurements of reflection and transmission of unpolarized light at near normal incidence for a variety of photocathodes over a range of wavelengths. Two of the cathodes were bialkali K_2CsSb and the experimental data for these, labelled B1 and B3 by Timan, are reproduced in Table 3 (Ref. [4] is not now readily accessible). The measurements are the so-called "three intensities": i) R_f the front face reflection from the cathode = R_3 in the notation of Fig. 2, ii) R_v the vacuum face reflection from the cathode which in Fig. 2 = R_3 with n_2 and n_4 interchanged, and iii) T the transmission through the cathode = T_3 of Fig. 2.

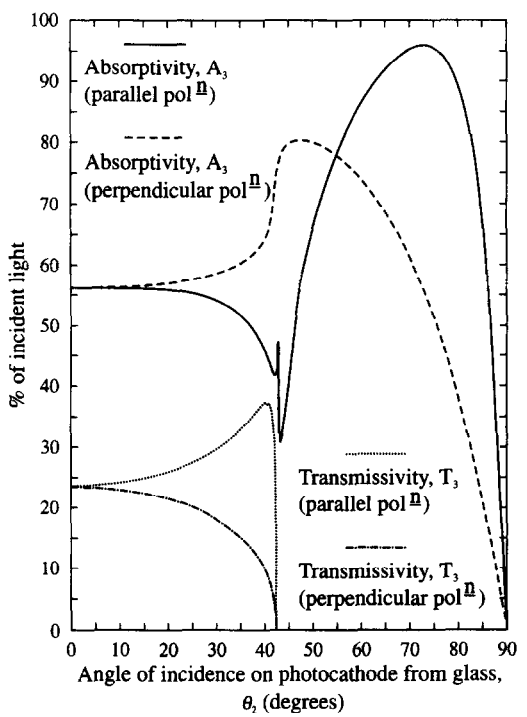

Fig. 6. Calculated angular and polarization dependences of the absorptance, A_3, and transmittance, T_3, of a K_2CsSb photocathode assuming the EMI 9124B parametrisation: $n_2 = 1.49$, $n_3 = 2.7$, $k_3 = 1.5$, $d = 23$ nm and $\lambda_0 = 442$ nm.

As presented in Table 3 the three intensities have been corrected for reflection losses at all air/glass boundaries. For a given wavelength the three intensities, fitted with the same Fresnel formulae [10] as used in Section 3, can in principle determine n_3, k_3 and d. In practice there are a large number of equally good fits and the ambiguity is *not* resolved by analysing all wavelengths measured and requiring the same thickness d for the same photocathode. The RMS errors of the fit of 2 to 4% allow too much freedom.

The ambiguity problem can be resolved by requiring the complex refractive index of Timan's B1 and B3 photocathodes to be as close as possible, at $\lambda_0 = 442$ nm, to the EMI 9124B parametrisation obtained in Section 3. There is substantial evidence [11] that different manufacturers obtain similar refractive indices for alkali antimonides, and Timan refers to a QE of 27% for a K_2CsSb cathode which would not shame EMI with a contemporary photomultiplier.

With some hesitation and reservations the ambiguity has been resolved by choosing the fit to Timan's measurement at 453 nm for the B1 and B3 to be as close as possible to the measured refractive index of EMI 9124B, which effectively fixes the thickness of the B1 and B3 cathodes and permits the evaluation of the refractive indices at other wavelengths. The parameters at 453 nm were as follows: $\tilde{n}_3 = 3.2 + i1.5$ and $d = 24$ nm for B1, and $\tilde{n}_3 = 3.25 + i1.5$ and $d = 29$ nm for B3.

The variation of real and imaginary parts of the refractive index with wavelength is shown in Fig. 7, where the size of the error bars have been chosen to reflect the uncertainty in the above "thickness fixing" procedure and also to show that at 390 nm there is still a considerable range of acceptable fits even after fixing the photocathode thickness.

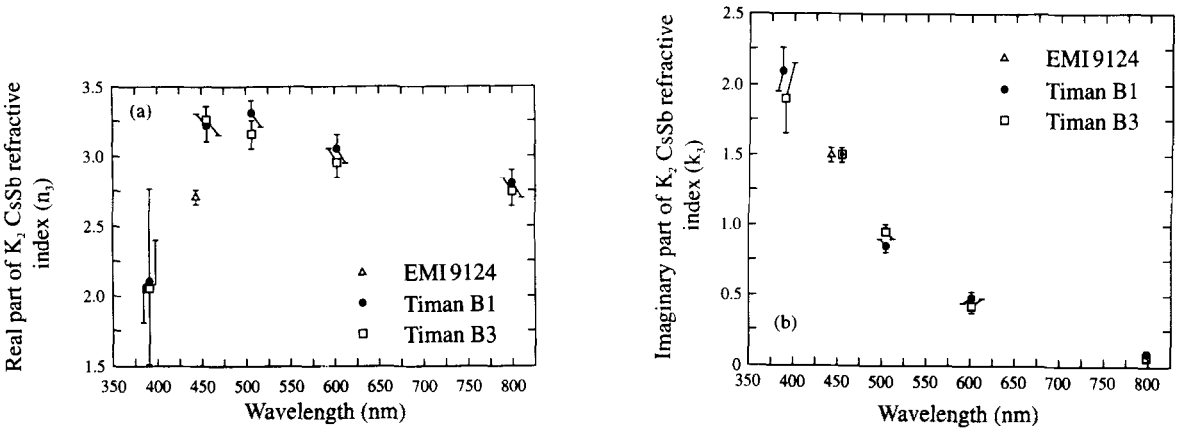

Fig. 7. Wavelength dependence of the K_2CsSb complex refractive index from the EMI 9124B parametrisation obtained in Section 3 and the re-analysis of Timan's measurements [4]: (a) real part (n_3), and (b) imaginary part (k_3).

5. Optical behaviour of photomultipliers with K_2CsSb photocathodes

The optical properties that shall be discussed are the photocathode's reflectance, transmittance and absorptance as a function of angle of incidence at the photomultiplier window (θ_1), refractive index of the medium in contact with the photomultiplier window (n_1), refractive index ($\tilde{n}_3$) and thickness (d) of the photocathode, and vacuum wavelength (λ_0). To simplify the discussion, polarization dependence has been ignored and all intensities in this section are the average of the calculated TE and TM intensities, i.e. unpolarized light is assumed.

In order to calculate the *total* reflectance, transmittance and absorptance of the front window of a photomultiplier one must sum (incoherently) the geometrical series of the multiple reflections inside the window (see Fig. 2). The resulting intensities (respectively R_{FW}, T_{FW} and A_{FW}) are given by

$$R_{FW} = R_{12} + \frac{R_3(T_{12})^2}{1 - R_{12}R_3}, \tag{1}$$

$$T_{FW} = \frac{T_{12}T_3}{1 - R_{12}R_3}, \tag{2}$$

$$A_{FW} = \frac{A_3T_{12}}{1 - R_{12}R_3}, \tag{3}$$

where R_{12}, T_{12}, R_3, T_3 and A_3 are the same quantities as in Section 3.

5.1. Influence of surrounding medium on angular behaviour

The medium which surrounds the photomultiplier influences the angular behaviour through refraction at the boundary between this medium (n_1) and the photomultiplier's glass window (n_2), see Fig. 2. This refraction determines the accessible range of angles at the photocathode (θ_2). As we have already seen in Fig. 6, the behaviour of the photocathode changes dramatically once θ_2 exceeds the angle for total internal reflection at a cathode/vacuum boundary, $\theta_2(c) = \sin^{-1}(1/n_2) = 42.2°$.

If $n_1 = 1.0$ (e.g. a photomultiplier in air) then the refraction at the n_1/n_2 boundary is such that θ_2 never exceeds $\theta_2(c)$ and so the resultant angular behaviour is flat. This is shown in Fig. 8a where we have assumed the EMI 9124B photocathode parametrisation obtained in Section 3, i.e. the values $n_2 = 1.49$, $n_3 = 2.7$, $k_3 = 1.5$, $d = 23$ nm. The cut-off in A_{FW} and T_{FW} at large angles is due to reflectivity at the n_1/n_2 boundary.

If $n_1 > 1.0$ then θ_2 can exceed $\theta_2(c)$ and the angular behaviour is more complicated. A common case for neutrino detectors is immersion in water ($n_1 = 1.34$). This case is shown in Fig. 8b, again assuming the EMI 9124B photocathode parametrisation obtained in Section 3. The angular behaviour is clearly divided into two regions separated by the angle for total internal reflection at the cathode/vacuum boundary, $\theta_1(c) = \sin^{-1}(1/n_1) = 48.3°$. Another frequent case is that of a photomultiplier in contact with a liquid or plastic scintillator of refractive index $n_1 \simeq 1.49$. In this case, the angular behaviour is practically identical to that shown in Fig. 8b except that the critical angle $\theta_1(c)$ is 42.2° instead of 48.3°.

One final case has to be considered: a photomultiplier in contact with a medium of higher refractive index than the glass. In this case there are two critical angles. The first is the angle $\theta_1(c)$ which has been discussed above, and the other is the critical angle for total internal reflection at the n_1/n_2 boundary, $\theta_1'(c) = \sin^{-1}(n_2/n_1)$. Clearly, at angles $\theta_1 \geq \theta_1'(c)$ no light is able to reach the photocathode and $R_{FW} = 1.0$. Thus the behaviour shown in Fig. 8b is compressed within the angle $\theta_1'(c)$.

In many photomultipliers, particularly the larger hemispherical photomultipliers of neutrino detectors, a significant fraction of the light transmitted by the photocathode (T_{FW})

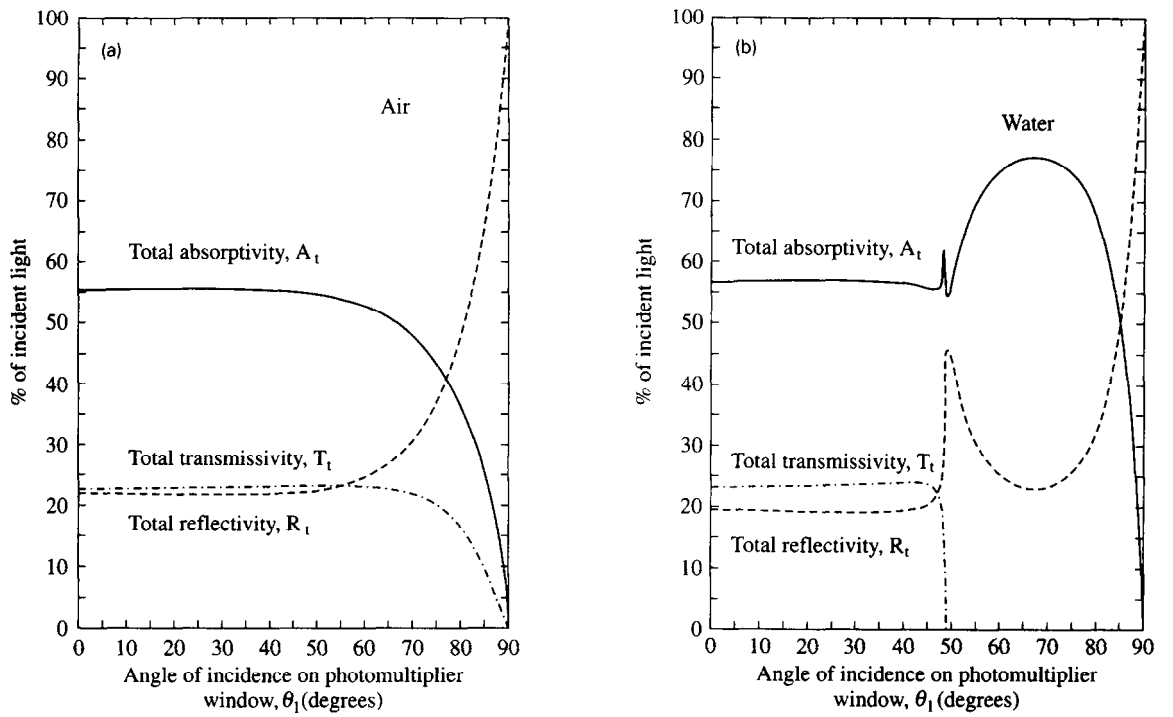

Fig. 8. Calculated polarization averaged front window absorptance, A_{FW}, reflectance, R_{FW}, and transmittance, T_{FW}, as a function of the angle of incidence at the photomultiplier, assuming that the photomultiplier window is in contact with: (a) air ($n_1 = 1.0$), and (b) water ($n_1 = 1.34$). In both cases the EMI 9124B parametrisation is assumed: $n_2 = 1.49$, $n_3 = 2.7$, $k_3 = 1.5$, $d = 23$ nm and $\lambda_0 = 442$ nm.

is reflected back onto the photocathode by aluminised internal surfaces. Ray-tracing simulations of the complicated internal geometry of EMI and Hamamatsu 20 cm photomultipliers indicate that $\sim 50\%$ of the T_{FW} intensity is eventually absorbed by the photocathode. These estimates have been corroborated by tests at EMI [12] using 20 cm photomultipliers with and without the internal aluminisation. Thus, by adding half of T_{FW} to A_{FW} one can estimate the *total* photocathode absorptance for the photomultiplier as a whole. It is clear from Fig. 8b that by following this recipe one obtains a more uniform angular response.

5.2. *Variation of photocathode thickness and wavelength*

So far, we have only considered one possible parametrization of the photocathode. There is substantial evidence [11] that alkali-antimonide photocathodes have, in general, well defined stoichiometries which are reproducible in photomultiplier production. Thus one expects that the tube-to-tube variation in photocathode refractive index is not so great and certainly less than the expected variation in photocathode thickness which is much more difficult to control in production. This is precisely what Lang [8] and Lay [9] have found in their investigations of two EMI 9124 photomultipliers at 442 nm, (see Section 1, Table 1).

Let us, then, consider the variation of photocathode thickness first (keeping the wavelength fixed at 442 nm) and return later to the wavelength dependence of the refractive index. To simplify the presentation, we will restrict the discussion to the case $n_1 = 1.49$ (photomultiplier immersed in liquid scintillator) and to only two angles of incidence. The first angle, 10°, indicates the behaviour at near normal incidence, $\theta_1 < \theta_1(c)$, and the second angle, 65°, indicates the behaviour in the region of total internal reflection, $\theta_1 > \theta_1(c)$. Fig. 9 shows the quantities $R_{FW}(10°)$, $T_{FW}(10°)$, $A_{FW}(10°)$, $R_{FW}(65°)$ and $A_{FW}(65°)$ as a function of photocathode thickness for the EMI 9124B parametrisation obtained in Section 3. At near normal incidence, the absorptance exhibits a plateau from about 15 nm to 30 nm thickness, whereas at 65° incidence there is a broad asymmetric peak at about 13 nm.

As discussed at the end of Section 5.1, many photomultipliers have aluminised internal surfaces which reflect most of the transmitted light back onto the photocathode. The net effect is that the *total* absorptance is roughly equal to $A_{FW} + \frac{1}{2}T_{FW}$. If the near normal absorptance, $A_{FW}(10°)$, shown in Fig. 9 is corrected for this effect, it resembles quite closely the absorptance at large angles, $A_{FW}(65°)$, and even displays an absorptance peak at about 15 nm.

The optimum thickness for maximum quantum efficiency is, of course, not just determined by the thickness dependence of absorptance but also by the thickness dependence of the probability of photo-electrons escaping into the vacuum. Nevertheless, there is some indication from Fig. 9 that the optimum photocathode thickness is about 15 nm. This

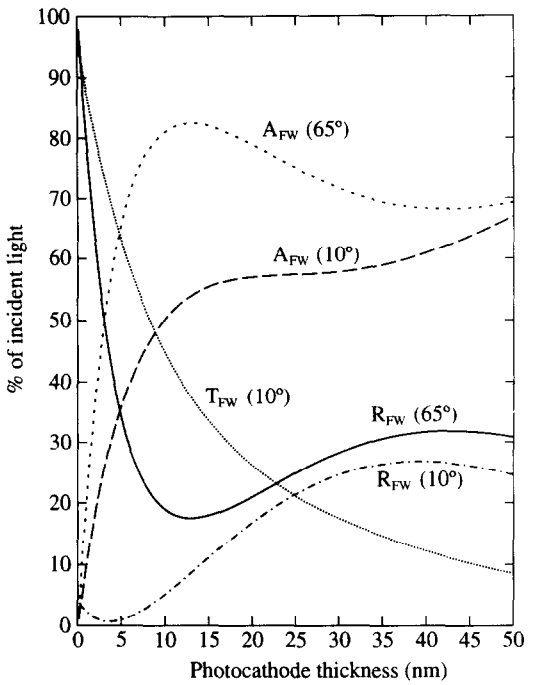

Fig. 9. Calculated thickness dependence of the polarization averaged front (water) window absorptance, A_{FW}, reflectance, R_{FW}, and transmittance, T_{FW}, at two angles of incidence (10° and 65°) for a photomultiplier in liquid scintillator (n_1 = 1.49) assuming the EMI 9124B parametrisation: n_2 = 1.49, n_3 = 2.7, k_3 = 1.5 and λ_0 = 442 nm.

is slightly less than the average thickness of the three well-characterized photomultipliers shown in Table 1.

In the thickness range 10–30 nm where the near normal absorptance is more-or-less constant, the transmittance and the near normal reflectance are quite strongly dependent on thickness. It is conceivable that either of these latter quantities could be used as on-line monitors for measuring photocathode thickness during production, e.g. a transmittance measurement of 33 ± 3% at 442 nm implies a photocathode thickness of 15 ± 1.8 nm, assuming the EMI 9124B parametrization. Obviously, this method will be susceptible to tube-to-tube variations in photocathode refractive index. However, if this variation is of the order of that found by Lang [8] and Lay [9] ($\leq$ ±5% variation in either n_3 or k_3) then the inferred thickness in the above example will have a systematic error of ±5%. This should be tolerable for the purposes of quality control during photomultiplier production, as current methods are based on the subjective determination of a trained operator.

Another interesting variation to consider is the wavelength dependence of the refractive index, as given by the re-analysis in Section 4 of Timan's data [4], (see Fig. 7). Several parametrizations, consistent with this re-analysis, were investigated at both λ_0 = 390 and 500 nm, either side of the much-studied 442 nm wavelength. It turns out that all of these investigated parametrizations have angular behaviours and thickness dependences which are very similar to those of the EMI 9124B parametrisation at 442 nm. The only significant differences are in the relative amounts of transmittance, reflectance and absorptance, as shown in Table 4, where at λ_0 = 500 nm there is somewhat more reflectance and transmittance and less absorptance that at either 442 or 390 nm.

6. Summary

The detailed measurement presented in Sections 2 and 3 of the angular and polarization dependence of the reflectance in water of a K_2CsSb photocathode allows an *unambiguous* determination of the photocathode's optical parameters. This reliable method of determining photocathode parameters is dependent on an accurate measurement of the reflectance peak which occurs for TM waves at the onset of total internal reflection, (see Figs. 4 and 5). For the particular photomultiplier investigated, EMI 9124B, the following values were obtained: thickness = 23 ± 2 nm and refractive index = 2.7 ± 0.1 + i(1.5 ± 0.1) at 442 nm wavelength. These results are consistent with those of Refs. [8] and [9] (see Table 1) where the same method was used to measure a pair of EMI 9125B photomultipliers.

The wavelength dependences of the real and imaginary parts of the K_2CsSb refractive index have been obtained by re-interpreting in Section 4 the "three intensities" data of Timan [4]. The inherent ambiguity from interpreting these data has been removed by assuming that the photocathodes measured by Timan have similar refractive indices to those of the EMI 9124B photomultiplier.

Using the EMI 9124B parametrisation and the wavelength dependence of the bialkali refractive index obtained in Section 4, the optical properties of photomultipliers with K_2CsSb photocathodes have been calculated as a function of: i) angle of incidence at the photomultiplier window, ii) refractive index of the medium in contact with the photomultiplier window, iii) photocathode thickness and iv) wavelength. The angular behaviour can be divided into two regions which are separated by the critical angle for total internal reflection at the cathode/vacuum boundary. In the region of total internal reflection the absorptance is slightly greater than at near normal incidence. Moreover, the optimum photocathode thickness for maximum absorptance is slightly smaller in the region of total internal reflection ($\sim$ 15 nm) than at near normal incidence ($\sim$ 20 nm). These small differences between the two angular regions are reduced in the case of photomultipliers with aluminized internal surfaces which reflect the transmitted light at near normal incidence back onto the photocathode.

It would be very valuable to obtain more parametrizations of K_2CsSb photocathodes across the wavelength range of reasonable quantum efficiency (300–550 nm) and with many tubes so as to determine more precisely the tube-to-tube variation in photocathode parameters. The method of determining photocathode parameters developed in this paper is ideal for this purpose.

Table 4
Calculated wavelength dependence of the polarization averaged front window absorptance, A_{FW}, reflectance, R_{FW}, and transmittance, T_{FW}, at two angles of incidence (10° and 65°) for a photomultiplier immersed in liquid scintillator (n_1 = 1.49) and with a bialkali photocathode of 20 nm thickness and the following refractive indices: i) n_3 = 2.1, k_3 = 2.0 at λ_0 = 390 nm, ii) n_3 = 2.7, k_3 = 1.5 at λ_0 = 442 nm, and iii) n_3 = 3.2, k_3 = 0.9 at λ_0 = 500 nm

Wavelength [nm]	$T_{FW}(10°)$	$R_{FW}(10°)$	$A_{FW}(10°)$	$R_{FW}(65°)$	$A_{FW}(65°)$
390	0.21	0.18	0.61	0.22	0.78
442	0.26	0.17	0.57	0.18	0.82
500	0.34	0.23	0.43	0.30	0.70

Acknowledgements

We would like to acknowledge the help of A. Ferraris in writing some of the computer programs used in the data analysis, R. McAlpine and J. Wardley for kindly lending us the EMI 9124B photomultiplier and for providing much general advice on photomultipliers, R. Smith who corrected a few errors in some of our equations and M. Lay who noticed a small error in one of the analysis routines.

The authors gratefully acknowledge the support of the U.K. Science and Engineering Research Council.

References

[1] R.J. Boardman, Ph.D. Thesis, Oxford University (1992).
[2] G.T. Ewan, Nucl. Instr. and Meth. A 314 (1992) 373.
[3] G. Doucas et al., Nucl. Instr. and Meth. A 370 (1995) 579.
[4] H. Timan, Optical characteristics and constants of high efficiency photoemitters, Revue Technique Thomson-CSF 8 (1976) 49.
[5] W. Greschat, H. Heinrich and P. Romer, Adv. Electronics and Electron Phys. A 40 (1976) 397.
[6] T.H. Chyba and L. Mandel, J. Opt. Soc. Am. B 5 (1988) 1305.
[7] M.E. Moorhead and N.W. Tanner, Optical properties of the K–Cs bialkali photocathode, Oxford University Preprint OUNP-91-95 (1991);
M.E. Moorhead, Ph.D. Thesis, Oxford University (1992).
[8] T. Lang, Photocathode Characterization, Thorn EMI Research Report X.2818/1A (1993).
[9] M. Lay, Ph.D. Thesis, Oxford University, unpublished, 1993; Parametrisation of the angular response of one inch photomultiplier tubes, Appl. Opt., to be published.
[10] M. Born and E. Wolf, Principles of Optics, 5th Ed. (Pergamon, 1975) Section 13.4.1, p. 628–631. Prof. R. Smith drew to our attention a misprint in Eq. (24) of Section 13.4.1 which was found in the 1st edition (1959) and which has been corrected in all subsequent editions.
[11] A.H. Sommer, Photoemissive Materials (Robert E. Kreiger, New York, 1980).
[12] R. McAlpine and J. Wardley, Thorn EMI, private communication, 1992.